Many-body interactions in colloidal suspensions

J Dobnikar[1]**, Y Chen**[1,3]**, R Rzehak**[2] **and H H von Grünberg**[1]

[1] Universität Konstanz, Fachbereich Physik, D-78457 Konstanz, Germany
[2] Institut für Festkörperforschung, Forschungszentrum Jülich, D-52425 Jülich, Germany
[3] Department of Physics, Lanzhou University, Lanzhou, Gansu, 730000, China

E-mail: jure.dobnikar@uni-konstanz.de

Abstract
At low ionic strength the interaction between any two charged colloids in a
concentrated charge-stabilized suspension is strongly influenced by the charge
distributions of other colloids in the neighbourhood of the two interacting
colloids. When such many-body interactions become important, a colloidal
suspension can no longer be treated as a simple Yukawa liquid. We here
(i) discuss experimental data showing that many-body interactions are indeed
present in low-salt-content colloidal suspensions, (ii) report on three-body
calculations in colloidal systems that help in understanding the concept
of 'macroion shielding', (iii) demonstrate the configuration dependence of
effective forces and (iv) illustrate, using simulations based on (a) a truncated
Yukawa potential with a density-dependent cut-off and (b) a full Poisson–
Boltzmann mean-field description, the effect of many-body interactions on the
solid–liquid phase behaviour of colloidal suspensions.

1. Introduction

The Derjaguin–Landau–Verwey–Overbeek (DLVO) theory [1] predicts a repulsive Yukawa-
like effective potential between a pair of charged colloids at large intercolloidal distances, a
prediction that has recently been confirmed by direct experimental measurements [2]. Also
for charge-stabilized colloidal suspensions, the DLVO theory, though originally dealing with
the effective interaction between two and just two colloids, correctly describes colloidal
interactions, but only under high-salt conditions and/or at low colloid volume fractions (weak
Coulomb coupling). In concentrated suspensions and at low salt concentrations, however, a
reduced description in terms of pairwise-additive Yukawa potentials is bound to fail, because
now the charges of other colloidal particles in the neighbourhood of two interacting colloids
will influence their mutual interaction. Such many-body interactions have turned out to play a
vital role in, for example, the recently proposed volume-term theories of the gas–liquid phase
behaviour of colloidal suspensions [3].

We here consider colloidal suspensions in those regions of the parameter space where they
can no longer be treated as a simple Yukawa liquid, and discuss some of the effects which
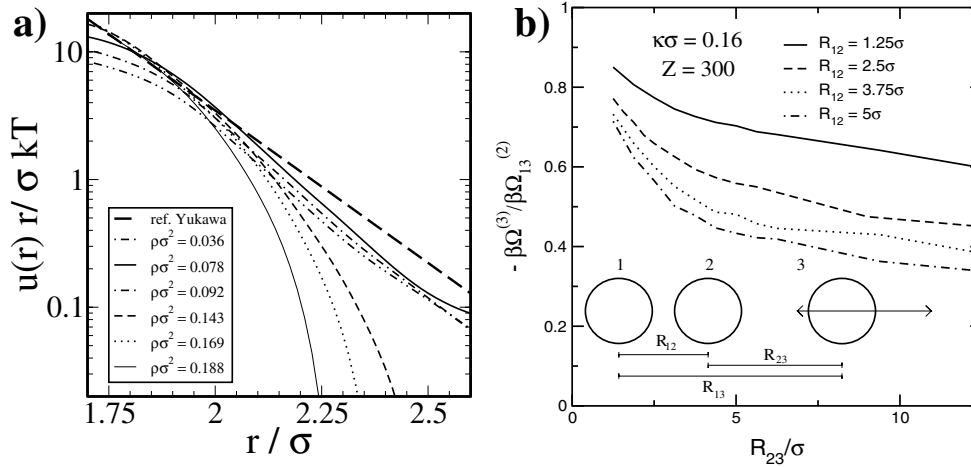
Figure 1. (a) Effective colloid–colloid pair potentials $u(r)$, obtained by inverting experimentally measured pair distribution functions in 2D colloidal systems [4]. As the inversion method, we here used the inverse MC method. Potentials are multiplied by r and plotted logarithmically, for different colloid densities ρ as indicated ($\sigma = 2a$, the diameter of a colloidal sphere). The thick curve corresponds to a reference Yukawa potential. (b) The ratio $-\Omega^{(3)}/\Omega^{(2)}(R_{13})$ of the collinear three-body potentials and the negative of the pair interaction $\Omega^{(2)}(R_{13})$ of the two outer spheres (labelled 1 and 3) [7]. The colloidal charge is $Z = 300$; the reservoir salt density $\kappa\sigma = 0.16$. The grand potential is computed after the full nonlinear PB equation is solved in three dimensions for three colloidal spheres in a row. In the case of perfect macroion shielding of the two outer particles by the central one, this ratio would take the value unity.

many-body interactions between the colloids can have on the effective intercolloidal potentials and the solid–liquid phase behaviour.

2. Many-body interactions in 2D colloidal systems

Recently, effective interparticle potentials in a two-dimensional (2D) charge-stabilized colloidal system have been systematically measured at different colloid densities ρ [4, 5]. Restriction to 2D is convenient as it allows one to determine colloidal positions by means of video-microscopy in a straightforward manner. From these positions, one can directly obtain the radial pair distribution function $g(r)$. Effective potentials $u(r)$ between the colloidal particles are determined by deconvoluting the information contained in $g(r)$, using appropriate inversion routines. Figure 1(a) shows the resulting potentials, plotted such that Yukawa potentials appear as straight lines. For the three lowest densities, one observes potentials very close to Yukawa form, just as standard DLVO theory predicts. For increasing density, however, $u(r)$ is Yukawa-like only at very short distances and shows clear and systematic deviations from the Yukawa form at larger distances. Working at a fixed salinity, these potentials would not depend on the colloid density if the interactions between the colloids were purely pairwise additive. A density dependence of the pair potential means that the mutual interaction of two colloidal particles depends on their local environment: two colloids isolated in an unbound electrolyte interact differently to two colloids at the same distance and at the same salinity but in a highly concentrated suspension. It is important to appreciate that many-body interactions, when included into what is an effective pair potential, lead to a density dependence of this pair potential [6]. Therefore, the density dependence of the pair potential recognizable in figure 1(a) is a direct experimental observation of many-body interactions in colloidal suspensions.

3. Three-body interactions and the macroion shielding effect

Assuming that the difference between the Yukawa-like potential and the measured pair potential in figure 1(a) arises mainly from three-body terms, we try to determine the latter approximately. To this end, we consider the grand potential $\Omega(\{R^N\})$ for the microions in the field created by N macroions in a chosen fixed colloidal configuration $\{R^N\}$. The grand potential can be calculated once we have solved the nonlinear Poisson–Boltzmann (PB) equation which provides us with the electrostatic potential $\Phi(r)$. If $N = 1$, the grand potential is just the self-energy of the colloidal particle, Ω_1. For two particles, $N = 2$, at a distance R_{12}, we have $\Omega_2(R_{12}) = 2\Omega_1 + \Omega^{(2)}(R_{12})$, where $\Omega^{(2)}(R_{12})$ is the pair interaction potential. Having three particles in the configuration, the grand potential is $\Omega_3(R_1, R_2, R_3) = 3\Omega_1 + \Omega^{(2)}(R_{12}) + \Omega^{(2)}(R_{13}) + \Omega^{(2)}(R_{23}) + \Omega^{(3)}(R_1, R_2, R_3)$ where the pair potentials are taken from the previous step where $N = 2$, and where the last term, $\Omega^{(3)}(R_1, R_2, R_3)$, is the three-particle interaction potential. This procedure for determining three-body potentials in colloidal suspensions has recently been realized for certain sets of macroion positions [7]; see also [8]. The simplest such macroion configuration is one where the centres of the colloids are on a straight line. Keeping the distance R_{12} constant and varying R_{23}, where particle 2 is between particles 1 and 3 (see figure 1(b)), the (attractive) three-body potential $\Omega^{(3)}$ goes to zero monotonically with R_{23}. To compare the magnitude of $\Omega^{(3)}$ with that of the pair interactions $\Omega^{(2)}$ between the two outer particles, we plot in figure 1(b) the ratio $-\Omega^{(3)}/\Omega^{(2)}(R_{13})$ as a function of R_{23}, for four different values of R_{12}. One concludes from this figure that the three-body potential equals a considerable fraction of the negative of the pair interaction between the two outer particles (up to 90% at R_{12}, $R_{23} \simeq \sigma$!). This means that the middle colloid essentially shields (or 'screens') the two outer ones from each other. In other words, the DLVO-like repulsive interaction between a pair of macroions is strongly reduced or even almost cancelled when another macroion lies somewhere in between. Generalizing this finding to a suspension of many macroions, it can be expected that the effect of three-particle interactions will be to modify the effective (i.e. density-dependent) pair potential at distances larger than the mean interparticle separation $d_m = \rho^{-1/3}$. Now, it is just in this distance regime in which the 'cut-off'-like deviations of the measured $u(r)$ in figure 1(a) from the Yukawa form are found. This suggests that this cut-off behaviour is due to the macroion shielding effect: two colloids separated by a distance $r > d_m$ will experience the screening effect of a third colloid, being very probably located somewhere between them. At $r < d_m$, on the other hand, no such third particle can block the colloid–colloid interaction; the interaction is determined by the microions alone and the pair potential is Yukawa-like. Of course, the macroion screening is not important if enough salt is present, since in this case the pair potential has decayed essentially to zero for $r \geqslant d_m$ due to microion screening.

4. Effective force calculations in 3D crystalline configurations

One may wonder whether macroion shielding plays a role also in 3D colloidal systems. To clarify this question, we have performed effective force calculations for colloids in 3D suspensions. To this end, we considered a fixed configuration (either FCC or BCC) of N colloidal spheres of radius a inside a cubic box with periodic boundary conditions, solved the multi-centred PB equation to determine the electrostatic potential in the region between the colloidal spheres and deduced the total force on each colloid by integrating the stress tensor over a surface enclosing the respective particle. While correlations between the microions are neglected in this approach, many-body interactions between the colloids are fully included. To numerically solve the PB equation, we followed Fushiki [11] and used N spherical coordinate
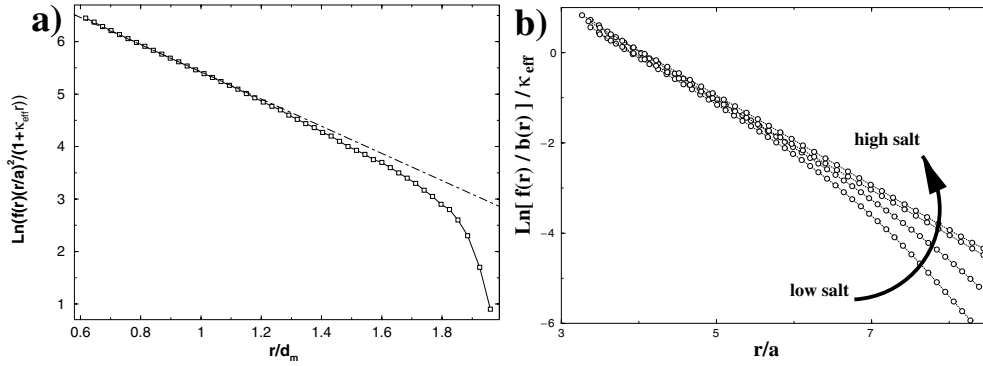
Figure 2. (a) Effective colloid–colloid force as a function of the distance between two colloids surrounded by 106 other colloids in a FCC configuration at volume fraction $\eta = 0.03$, colloidal charge $Z = 1000$, salt concentration $\kappa a = 0.2$ and Bjerrum length $\lambda_B/a = 0.012$. The dot–dashed line is the best-fitting Yukawa interaction. Data are plotted in such a way that a Yukawa pair force transforms into a straight line with the slope $-\kappa_{\text{eff}}$. (b) Effective force curves in a FCC configuration for different salt concentrations ($\kappa a = 0.1, 0.2, 1.0, 2.0$; other parameters as in figure 1(a)). The calculated forces $f(r)$ are divided by $b(r) = [Z_{\text{eff}} e^{\kappa_{\text{eff}} a}/(1 + \kappa_{\text{eff}} a)]^2 \frac{\lambda_B}{a}(1 + \kappa_{\text{eff}} r)/(r/a)^2$, the logarithm taken and the result divided by κ_{eff}, so a Yukawa pair force following the DLVO theory, $f_{\text{DLVO}}(r) = b(r) e^{-\kappa_{\text{eff}} r}$, appears as a straight line with the slope -1.

systems—centred on the colloids—together with a Cartesian system in the cubic simulation box. To derive effective forces, we considered the force $\vec{\mathcal{F}}_{AB}$ exerted by particle A on particle B which is obtained as the difference between the total force acting on particle B with particle A present, $\vec{\mathcal{F}}_B^1$, and the total force acting on particle B, $\vec{\mathcal{F}}_B^0$, after removing particle A while leaving all other particles at their positions. Varying the position of particle A results in the effective force curve $\vec{\mathcal{F}}_{AB}(\vec{r}) = \vec{\mathcal{F}}_B^1(\vec{r}) - \vec{\mathcal{F}}_B^0$ where $\vec{r}$ is the distance vector between A and B. With this procedure, many-body interactions, if present, are folded into an effective pair force curve. A typical effective force curve $\vec{f}(r) = a\vec{\mathcal{F}}_{AB}(r)/kT$ resulting from such a calculation is presented in figure 2(a). We observe a perfect Yukawa-like behaviour at small distances, but systematic deviations starting around the mean distance d_m and developing into a cut-off at a distance $r \approx 1.9 d_m$. Figure 2(b) compares the effective force curves to the predictions of DLVO theory, for different salt concentrations: the cut-off feature, observable under low-salt conditions, vanishes at high ionic strength ($\kappa a = 2.0$) where perfect agreement with the predictions of DLVO theory is observed at all distances probed. The values of the parameters κ_{eff} and Z_{eff} needed here were obtained by fitting the effective force curves to a Yukawa potential at small distances where the force is perfectly Yukawa-like. Performing the fitting procedure for all calculated force curves enables us to determine the dependence of κ_{eff} and Z_{eff} on the state of the system ($\kappa a, Z, \eta$). This can be done for effective force curves based on the FCC and BCC configurations of the colloids. Comparing these functions, e.g. $Z_{\text{eff}}^{\text{BCC}}(Z)$ and $Z_{\text{eff}}^{\text{FCC}}(Z)$, we found a systematic configuration dependence of the effective parameters: quite small at high ionic strength ($\kappa a = 2.0$), but becoming appreciable on reducing the salt concentration to $\kappa a = 0.2$. This can be observed also in figure 3(a). A similar dependence of the pair interaction on the colloidal configurations has been found in [12]. It is important to realize that if the interactions in the system were pairwise additive, the resulting effective interaction would by construction be identical to the presupposed pairwise interaction potential, no matter how the surrounding particles (all particles but A and B) are arranged. Together with the cut-off feature, the configuration dependence of the effective interaction is thus a
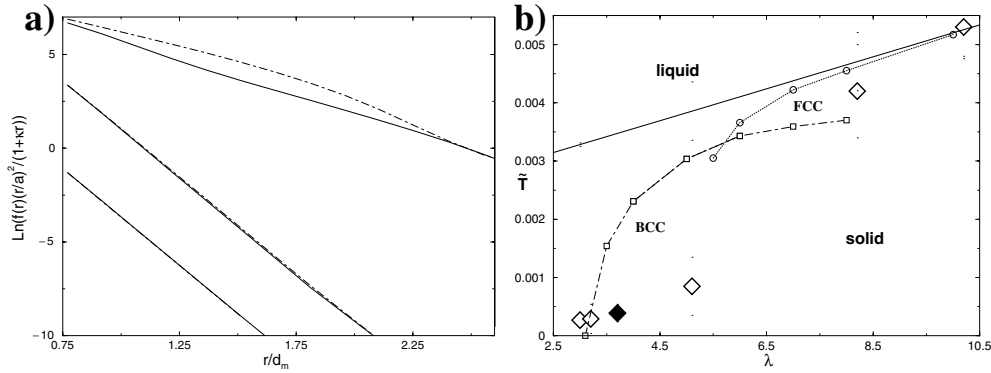
Figure 3. Effective force curves as in figure 2(a), calculated by analysing a FCC configuration (dot–dashed curves) and a BCC configuration (solid lines) at the same volume fraction ($\eta = 0.03$). The lower two curves are for a colloidal charge $Z = 100$ and a salt concentration $\kappa a = 2.0$ ('high salt'), the middle ones for $Z = 2000$ and $\kappa a = 2.0$, the upper pair for $Z = 2000$ and $\kappa a = 0.2$ ('low salt'). Other parameters are as in figure 2(a). No configuration dependence is observed for the high-salt case (lower and middle pairs of curves), while clearly in the low-salt case the forces depend on the configuration. (b) The solid–liquid phase diagram of a charge-stabilized colloidal suspension, spanned by the reduced temperature $\tilde{T}$ and the ratio of the mean distance and the screening length $\lambda = \kappa d_m$. We show: the melting line of a pure Yukawa system obtained by Robbins *et al* [9] (solid line); the melting line obtained assuming Yukawa interactions with a density-dependent cut-off after the first-neighbour shell in a FCC configuration (dotted curve) and in a BCC configuration (dot–dashed curve); and data from numerical simulations combining a PB treatment and a molecular dynamics simulation technique (large symbols) [10].

clear fingerprint of many-body interactions becoming important in low-salt-content colloidal systems.

5. The effect of macroion shielding on the solid–liquid phase behaviour

From our earlier discussion we infer that the observed cut-off feature of the force curves in figures 2(a) and (b) is due to macroion shielding. Guided by this finding, we here propose to model the effective pair force between colloids in suspensions by

$$
-\frac{\mathrm{d}u(r)}{\mathrm{d}r} = \begin{cases} U_0/d_m \dfrac{\mathrm{e}^{-\lambda r/d_m}}{(r/d_m)^2}(1 + \lambda r/d_m) & r \leqslant r_c \\ 0 & r > r_c, \end{cases} \tag{1}
$$

with a prefactor U_0, a screening constant λ and a *density-dependent* cut-off $r_c \propto d_m = \rho^{-1/3}$. Through this density-dependent cut-off, the many-body interactions are included (to some extent, at least) in the pair potential. Using this model potential, we carried out MD simulations and determined the solid–liquid phase boundary from the Lindemann melting criterion, computing the rms displacement for various combinations of U_0 and λ in FCC and BCC crystals and for cut-offs directly behind the first-, second-, third-neighbour shells. For a system of point-like Yukawa particles, interacting via $u(r) = U_0 \mathrm{e}^{-\lambda r/d_m}/(r/d_m)$, Robbins, Kremer and Grest (RKG) [9] determined the melting line, that is, the function $U_0^M(\lambda)$. More precisely, they introduced an effective temperature (kT in units of the Einstein phonon energy) and determined $\tilde{T}_M(\lambda) = 0.002\,46 + 0.000\,274\lambda$, a function that is directly related to the prefactor at melting $U_0^M(\lambda)$; see [9]. The RKG melting line is plotted in figure 3(b) as a solid line. For $r_c = 3.07d_m$ (the cut-off used in [9] for numerical reasons), we were able

to reproduce the RKG melting line using the pair force in equation (1). Decreasing the cut-off then, we observed systematic deviations from the RKG melting line occurring first at small values of λ. The dotted curve (dashed–dotted curve) in figure 3(b) is the melting line obtained choosing $r_c = 1.35d_m$ ($r_c = 1.50d_m$) in a FCC (BCC) configuration. Such phase behaviour of the simple model system (1) is compared to a full MD–PB simulation (symbols in figure 3(b)) where a technique has been used combining a continuous PB description for the microscopic electrolyte ions with a MD simulation for the macroionic colloidal spheres [10]. This simulation accounts for all macroionic many-body effects. The simulation results show good agreement with RKG ones if obtained under high-salt conditions $\kappa a = 2.0$ ($\lambda \approx 10$), which is consistent with our finding that at high salt content neither a cut-off behaviour nor a configuration dependence of the pair potential could be observed. Obviously, in this salt regime the colloidal suspension can be represented quite well by a Yukawa system. However, reducing the amount of salt, i.e., decreasing λ, we observe pronounced deviations from the RKG line. Again, this matches with the behaviour of the calculated effective force curves at low salt content, showing a configuration dependence but also the cut-off feature. From the reasonable agreement of our full MD–PB simulation results with the truncated Yukawa results, it becomes clear that modelling colloidal interactions by truncated Yukawa potentials with a density-dependent cut-off provides a considerable improvement over using the plain Yukawa potential, as regards the phase behaviour.

Acknowledgments

References

[1] Verwey E J W and Overbeek J T G 1948 *Theory of the Stability of Lyophobic Colloids* (New York: Elsevier)
[2] Crocker J C and Grier D G 1994 *Phys. Rev. Lett.* **73** 352
[3] Beresford-Smith B, Chan D Y C and Mitchell D J 1985 *J. Colloid Interface Sci.* **216** 9691
    van Roij R, Dijkstra M and Hansen J-P 1999 *Phys. Rev.* E **59** 2010
    Denton A R 2000 *Phys. Rev.* E **62** 3855
    von Grünberg H H, van Roij R and Klein G 2001 *Europhys. Lett.* **55** 580
    Petris S N and Chan D Y C 2002 *J. Chem. Phys.* **116** 8588
[4] Klein R, von Grünberg H H, Bechinger C, Brunner M and Lobaskin V 2002 *J. Phys.: Condens. Matter* **14** 7631
[5] Brunner M, Bechinger C, Strepp W, Lobaskin V and von Grünberg H H 2002 *Europhys. Lett.* **58** 926
[6] Louis A A 2002 *J. Phys.: Condens. Matter* **14** 9187
[7] Russ C, van Roij R, Dijkstra M and von Grünberg H H 2002 *Phys. Rev.* E **66** 011402-1
[8] Löwen H and Allahyarov E 1998 *J. Phys.: Condens. Matter* **10** 4147
    Wu J Z, Bratko D, Blanch H W and Prausnitz J M 2000 *J. Chem. Phys.* **113** 3360
[9] Robbins M O, Kremer K and Grest G S 1988 *J. Chem. Phys.* **88** 3286
[10] Dobnikar J, Rzehak R and von Grünberg H H 2002 *Preprint* cond-mat 0209162
[11] Fushiki M 1992 *J. Chem. Phys.* **97** 6700
[12] Löwen H and Kramposthuber G 1993 *Europhys. Lett.* **23** 673